

Tumor cell apoptosis induces tumor-specific immunity in a CC chemokine receptor 1- and 5-dependent manner in mice

メタデータ	言語: English 出版者: 公開日: 2017-11-09 キーワード: 作成者: Iida, Noriho, Nakamoto, Yasunari, Baba, Tomohisa, Kakinoki, Kaheita, Li, Ying-Yi, Wu, Yu, Matsushita, Kouji, Kaneko, Shuichi, Mukaida, Naofumi, 中本, 安成, 馬場, 智久, 金子, 周一, 向田, 直史 メールアドレス: 所属:
URL	https://doi.org/10.24517/00027539

This work is licensed under a Creative Commons Attribution-NonCommercial-ShareAlike 3.0 International License.



Tumor Cell Apoptosis Induces Tumor-Specific Immunity in a CC Chemokine Receptor 1- and 5-Dependent Manner in Mice

Noriho Iida,¹ Yasunari Nakamoto,¹ Tomohisa Baba,² Kaheita Kakinoki,¹ Ying-Yi Li,² Yu Wu,² Kouji Matsushima,³ Shuichi Kaneko¹ and Naofumi Mukaida²

¹Disease Control and Homeostasis, Graduate School of Medical Science, ²Division of Molecular Bioregulation, Cancer Research Institute, Kanazawa University, Kanazawa, Japan,

³Department of Molecular Preventive Medicine, School of Medicine, University of Tokyo, Tokyo, Japan

Running title: Chemokine-dependent establishment of specific tumor immunity

Key Words: Chemokines, Dendritic Cells, Gene Therapy, Tumor Immunity

Footnotes:

Address corresponding to: Naofumi Mukaida, M.D., PhD, Division of Molecular Bioregulation, Cancer Research Institute, Kanazawa University, 13-1 Takara-machi, Kanazawa 920-0934, Japan. Phone, 81-76-265-2767; Fax, 81-76-234-4520; E-mail, naofumim@kenroku.kanazawa-u.ac.jp

Nonstandard Abbreviations used in this paper:

BNL, BNL 1ME A.7R.1; BNL-tk, BNL cells transfected with HSV-tk gene; DC, dendritic cell; DLN, draining lymph node; GCV, ganciclovir; HSV-tk, herpes simplex virus –thymidine kinase; KO, knockout (deficient); WT, wild type.

ABSTRACT

The first step in the generation of tumor immunity is the migration of dendritic cells (DCs) to the apoptotic tumor, which is presumed to be mediated by various chemokines. In order to clarify the roles of chemokines, we induced apoptosis using suicide gene therapy and investigated the immune responses following tumor apoptosis. We injected mice with a murine hepatoma cell line, BNL transfected with herpes simplex virus-thymidine kinase (HSV-tk) gene and then treated the animals with ganciclovir (GCV). GCV treatment induced massive tumor cell apoptosis accompanied with intratumoral DC infiltration. Tumor-infiltrating DCs expressed chemokine receptors CCR1 and CCR5, while T cells and macrophages expressed CCL3, a ligand for CCR1 and CCR5. Moreover, tumor apoptosis increased the numbers of DCs migrating into the draining lymph nodes and eventually generated a specific cytotoxic cell population against BNL cells. Although GCV completely eradicated HSV-tk-transfected BNL cells in CCR1-, CCR5-, or CCL3-deficient mice, intratumoral and intranodal DC infiltration and the subsequent cytotoxicity generation were attenuated in these mice. When parental cells were injected again after complete eradication of primary tumors by GCV treatment, the wild-type mice completely rejected the rechallenged cells, but the deficient mice exhibited impairment in rejection. Thus, we provide definitive evidence indicating that CCR1 and CCR5, and their ligand CCL3 play a crucial role in the regulation of intratumoral DC accumulation and the subsequent establishment of tumor immunity following induction of tumor apoptosis by suicide genes.

INTRODUCTION

Hepatocellular carcinoma (HCC) occurs in individuals with chronic liver disease related to either hepatitis B or C virus infections (1-3). Even after the curative treatments for HCC, such as surgical resection and radiofrequency ablation, tumor recurrence often occurs because of the multicentric development of HCC in the cirrhotic liver (4). Immune-based therapies, particularly those based on dendritic cells (DCs), may be theoretically effective in preventing the recurrence because of their potential capacity to search for and eradicate tumor cells irrespective of site (5). However, DC-based therapy is still considered to be in its infancy probably due to the lack of effective techniques for enhancing the immune response to human cancer cells including HCC, which are generally poor in immunogenicity.

Apoptotic tumor cells are generally less immunogenic than necrotic cells, but they can sometimes induce efficient antitumor immune responses depending on the type of apoptosis inducer. Indeed, some anti-cancer drugs can induce apoptosis of tumor cells and simultaneously enhance the immunogenicity of apoptotic cancer cells (6-8). Ganciclovir (GCV) can activate the protease family of caspases and induce apoptosis selectively in the cells transfected with the herpes simplex virus-thymidine kinase (HSV-tk) gene (9, 10). Thus, when GCV is administered systemically to tumor-bearing individuals, it induces apoptosis of HSV-tk-transfected tumor cells but not normal cells. This treatment strategy, designated as suicide gene therapy, can induce immunogenic apoptosis of the tumor cells (11) as evidenced by a massive intra-tumoral infiltration of macrophages and T cells (12). Moreover, the expression of various pro-inflammatory cytokines is augmented at the tumor sites following GCV treatment (12, 13). Furthermore, in order to enhance the suicide gene therapy-induced immune responses, the simultaneous use of cytokines such as GM-CSF, IL-2, and MCP-1/CCL2 has been employed with some success (14-16). In order to design more effective methods of preventing tumor recurrences, it is necessary to fully understand the immune responses after tumor apoptosis induced by HSV-tk/GCV suicide gene therapy.

DCs are potent antigen-presenting cells (APC) that play a crucial role in the establishment of adoptive immune response. Immature DCs capture and process antigens at the inflammatory sites and thereafter migrate to the draining lymph node where they undergo

phenotypical and functional maturation. At the draining lymph node, the mature DCs interact with naïve T cells and present the captured and processed antigen to T cells (17, 18).

Chemokines are presumed to play an essential role in the regulation of DC trafficking and DC–T cell interaction in general (19-22). Circulating immature DCs express inflammatory chemokine receptors such as CCR1, CCR2, CCR5, and CCR6 and these DCs can reach the source of the inflammatory stimulus under the guidance of the ligand gradient for the expressed receptors such as CCL2, CCL3, CCL4, CCL5, CCL7, and CCL20. After capturing antigens, DCs undergo maturation, resulting in a decrease in inflammatory chemokine receptor expression and a reciprocal increase in CCR7 expression. Mature DCs expressing CCR7 migrate to T cell-rich areas of the draining lymph nodes where the ligands for CCR7, CCL19, and/or CCL21 are abundantly expressed. However, it still remains elusive whether similar mechanisms operate in the DC migration process following massive tumor apoptosis induced by treatments such as gene therapy, chemotherapy, and radiation therapy.

Here, we demonstrate the induction of specific tumor immunity by tumor apoptosis after HSV-tk/GCV suicide gene therapy and essential roles of DCs in this process. Moreover, we provide definitive evidence to indicate that both CCR1 and CCR5, and their ligand CCL3 play a key role in the regulation of intratumoral DC accumulation and the subsequent establishment of tumor immunity following induction of tumor apoptosis by HSV-tk/GCV suicide gene therapy. These observations might lay the foundation for devising novel measures to enhance antitumor immune responses in order to prevent tumor recurrence.

MATERIALS AND METHODS

Mice

Specific pathogen-free 7- to 9-week-old male BALB/c mice were purchased from Charles River Japan (Yokohama, Japan) and designated as wild-type (WT) mice. CCL3-deficient (CCL3KO) mice were obtained from Jackson Laboratories (Bar Harbor, ME). CCR1-deficient (CCR1KO) mice were a gift from Dr. Philip M. Murphy (NIAID, NIH, Bethesda, MD). CCR5-deficient (CCR5KO) mice were generated as previously described (23). All mice were backcrossed to BALB/c mice for 8 to 10 generations. All animal experiments were performed under specific pathogen-free conditions in accordance with the Guideline for the Care and Use of Laboratory Animals of Kanazawa University.

Tumor cell lines

A murine HCC cell line, BNL 1ME A.7R.1 (BNL), was cultured in Dulbecco's modified essential medium (DMEM) (Sigma Chemical Co., St. Louis, MO) containing 10% fetal bovine serum (FBS; Gibco, Long Island, NY). BNL cells were infected with the retroviral vector pG1Sv.Na harboring HSV-tk cDNA. The infected BNL cells were cultured in 10% FBS-containing DMEM in the presence of 400 µg/ml G418 (Gibco). The surviving cells were tested for sensitivity to GCV *in vitro* as described previously (24). GCV-sensitive cells were designated as BNL-tk and were used in the experiments.

Apoptosis detection assay

After culturing for 1 day with 5 µg/ml GCV, BNL-tk cells were harvested and phosphatidyl serine levels were determined by staining the cells with propidium iodide (PI) and the Annexin V-FITC Apoptosis Detection Kit (Calbiochem, Darmstadt, Germany) according to the manufacturer's instructions. At least 50,000 stained cells were analyzed on a FACSCalibur system (BD Biosciences, San Diego, CA) for each determination.

Tumor injection

Seven- to 9-week old male WT, CCR1KO, CCR5KO, and CCL3KO mice were inoculated

subcutaneously into the left flank with 2×10^5 BNL-tk cells on day 0. From days 14 to 18 (5 consecutive days), 75 mg/kg GCV (i.p.) was administered daily (Fig. 1C). Tumors were removed at the indicated time intervals for immunohistochemical analysis and quantitative real-time RT-PCR. In another series of experiments, WT, CCR1KO, CCR5KO, or CCL3KO mice were inoculated with 1.5×10^5 BNL-tk on day 0. The mice were intraperitoneally injected with 75 mg/kg GCV from days 2 to 5. The animals were then rechallenged subcutaneously with 1.0×10^5 BNL in their right flank on day 18, after confirming that the primary tumors were eradicated completely (Fig. 5A). Tumor sizes were evaluated twice a week using calipers and tumor volume was calculated by the following formula:

$$\text{Tumor volume (mm}^3\text{)} = (\text{the longest diameter}) \times (\text{the shortest diameter})^2/2$$

The draining lymph nodes (inguinal and axillary) were removed from the mice at the indicated time intervals for flow cytometric analysis and cytotoxicity assay.

Immunohistochemical analysis

Rabbit anti-mouse CCR5 polyclonal antibodies were prepared as described previously (25). The removed tumor tissues were embedded in paraffin or the Sakura Tissue-Tek OCT compound (Sakura Finetek, Torrance, CA) as frozen tissues. The paraffin-embedded sections were then stained with goat anti-mouse CCR1 (Santa Cruz Biotechnology, Santa Cruz, CA), rabbit anti-CCR5, goat anti-mouse CCL3 (R&D Systems, Minneapolis, MN), rat anti-mouse F4/80, anti-mouse CD3 (Serotec, Oxford, U.K.), rabbit anti-single stranded DNA, or rat anti-Ki67 (Dako Cytomation, Tokyo, Japan) overnight at 4°C. Cryostat sections of the frozen tissues were fixed with 4% paraformaldehyde (PFA) in PBS, and stained with rat anti-mouse DEC205 (Serotec) or hamster anti-mouse CD11c (BD Biosciences) overnight at 4°C. The sections were then incubated for 1 hour at room temperature with biotinylated rabbit anti-goat IgG, biotinylated swine anti-rabbit IgG, biotinylated rabbit anti-rat IgG (Dako Cytomation), or biotinylated mouse anti-hamster IgG (BD Biosciences). The immune complexes were visualized using a Catalyzed Signal Amplification System (Dako Cytomation) or the ELITE ABC and DAB Substrate Kits (Vector Laboratories, Burlingame, CA) except for anti-ssDNA, where a novel horseradish peroxidase-labeled polymer (Envision⁺, Dako Cytomation) was used according to the manufacturer's instructions. As a negative control, goat IgG (R&D Systems),

rabbit IgG (DAKO Cytomation), rat IgG (Cosmo Bio, Tokyo, Japan), or hamster IgG (BD Biosciences) was used instead of specific primary antibodies. The numbers of positive cells were determined in each animal in 10 randomly chosen fields at 400-fold magnification by an examiner without any prior knowledge of the experimental procedures.

Double-color immunofluorescence analysis

Tumor tissues were embedded in paraffin or the OCT compound as frozen tissues. The paraffin-embedded sections were then stained with combinations of rat anti-mouse CD3 and goat anti-mouse CCL3 or anti-F4/80 and anti-CCL3 antibodies overnight at 4°C. After fixation with 4% PFA/PBS, cryostat sections were stained with the combinations rat anti-mouse CD4 (BD Biosciences) and anti-CCR1, rat anti-mouse CD8a (BD Biosciences) and anti-CCR1, anti-CD4 and anti-CCR5, anti-CD8a and anti-CCR5, rat anti-DEC205 and anti-CCR1, anti-DEC205 and anti-CCR5, PE-conjugated hamster anti-CD11c (BD Biosciences) and anti-CCR1, PE-conjugated anti-CD11c and anti-CCR5, PE-conjugated anti-CD11c and rat anti-CD11b (BD Biosciences), or PE-conjugated anti-CD11c and anti-CD8a antibodies. After extensive washing, AF488 donkey anti-rat IgG (Invitrogen, Carlsbad, CA) was applied as the secondary antibody to detect CD4-, CD8a-, CD3-, F4/80-, DEC205-, or CD11b-positive cells. Simultaneously, AF546- or AF488-donkey anti-goat IgG (Invitrogen) was used to detect CCR1- or CCL3-positive cells, and AF594- or AF488-donkey anti-rabbit IgG (Invitrogen) was employed to detect CCR5-positive cells. The sections were observed using a confocal microscope (LSM 510 META, Zeiss, NY). The percentage of double-positive cells was determined in each animal in 5 randomly chosen fields at 400-fold magnification by an examiner without any prior knowledge of the experimental procedures.

Flow cytometric analysis

Inguinal and axillary lymph nodes were removed and digested in a DNase I and collagenase solution (Sigma). The resultant single cell preparations were stained with various combinations of FITC-labeled anti-CD4, FITC-labeled anti-CD86, PE-labeled anti-CD8, PE-labeled anti-CD11c, PE-labeled anti-CD44, and PE-labeled anti-CD62L monoclonal antibodies (BD Biosciences). FITC-rat IgG, PE-hamster IgG, and PE-rat IgG were used as isotype controls (BD

Biosciences). To prepare the tumor lysate, BNL or CT26 cells were suspended in PBS and subjected to four cycles of rapid freezing in liquid nitrogen and thawing at 55°C. The lysate was spun at 15,000 rpm to remove particulate cellular debris. In order to stain intracellular IFN- γ , the mononuclear cells harvested from the draining lymph nodes on day 8 (Fig. 5A) were incubated with the BNL or CT26 lysates at a tumor cell:mononuclear cell ratio of 1:1 in the presence of GolgiPlug (BD Biosciences). Six hours later, surface staining was performed with APC-conjugated CD8 antibodies. Intracellular IFN- γ was stained after fixation and permeabilization with BD Cytotfix/Cytoperm buffer with PE-conjugated IFN- γ antibodies or isotype control using the Mouse Intracellular Cytokine Staining Starter Kit (BD Biosciences). At least 100,000 stained cells were analyzed on a FACSCalibur system for each determination. The data were expressed as a proportion of positive cells (compared to cells stained with an irrelevant control antibody) and the absolute positive cell numbers were calculated after determining the total cell numbers in the lymph nodes by the following formula:

Absolute positive cell numbers = total cell number in the lymph nodes \times percentage of positive cells \times 1/100.

Quantitative real-time RT-PCR

Total RNA was extracted from the resected tumor and lymph nodes using RNA-Bee (Tel-Test, Friendswoods, TX) according to the manufacturer's instructions. After the RNA preparations were further treated with ribonuclease-free deoxyribonuclease (DNase) I (Life Technologies, Gaithersburg, MD) to remove residual DNA, cDNA was synthesized as described previously (26). Quantitative real-time PCR was performed on an Applied Biosystems StepOne™ Real-Time PCR System (Applied Biosystems, Foster, CA) using the comparative C_T quantification method. TaqMan® Gene Expression Assays (Applied Biosystems) containing specific primers (accession numbers: CCL3, Mm00441258_ml; CCL4, Mm00443111_m1; CCL5, Mm01302428_ml; CCR1, Mm00438260_s1; CCR5, Mm01216171_m1; GAPDH, Mm99999915_g1), TaqMan® MGB probe (FAM™ dye-labeled), and TaqMan® Fast Universal PCR Master Mix were used with 10 ng cDNA to detect and quantify the expression levels of CCL3, CCL4, CCL5, CCR1, and CCR5. Reactions were performed for 20 s at 95°C, then for 40 cycles of 1 s at 95°C and 20 s at 60°C. GAPDH was amplified as an internal control. C_T values

of GAPDH were subtracted from C_T values of the target genes (ΔC_T). ΔC_T values of tumors after GCV injection were compared to ΔC_T values of tumors before GCV injection.

Cytotoxicity assay

Mononuclear cells were isolated from the draining lymph nodes at the indicated time intervals and were incubated at a cell density of 2×10^6 cells/ml in the presence of 0.6×10^6 cells/ml BNL cells, which were irradiated at 50 Gy beforehand. After 5 days of culture, the cells were tested for cytotoxicity in an LDH assay using the CytoTox 96 Non-Radioactive Cytotoxicity Assay kit (Promega, Madison, WI) according to the manufacturer's instructions. Effector cells were added to target cells in triplicate at different E/T ratios. Percentage of specific lysis was calculated using the following formula:

$$[(\text{Experimental} - \text{Effector spontaneous} - \text{Target spontaneous}) / (\text{Target maximum} - \text{Target spontaneous})] \times 100\%.$$

Adoptive transfer of DC

Draining lymph nodes were harvested on day 8 as shown in Fig. 5A, and were digested with DNase I and collagenase solution. Mononuclear cells were obtained by centrifugation over a Histopaque-1077 density gradient (Sigma) and DCs were isolated by CD11c-conjugated magnetic microbeads (Miltenyi Biotec, Auburn, CA). CD11c-positive DCs (2.5×10^5 /mouse) were injected into the left flank of GCV-treated knockout mice on day 8 as shown in Fig. 5A. On day 18, DC-transferred mice were rechallenged with 1×10^5 BNL cells in their right flank, and tumor sizes were measured.

Statistical analysis

Data were analyzed statistically using one-way ANOVA followed by the Tukey–Kramer test, except for tumor progression data, which were analyzed using two-way ANOVA. Data of tumor sizes after adoptive transfer of DC experiment were analyzed using Mann-Whitney U test. $p < 0.05$ was considered statistically significant.

RESULTS

GCV treatment induces tumor cell apoptosis with intratumoral CCR1-, CCR5-, and CCL3-positive cell accumulation in WT mice

We investigated whether HSV-tk-GCV treatment can induce apoptosis *in vitro* in the tk-transfected murine hepatoma cell line BNL-tk. GCV treatment significantly increased the proportions of both early (annexin-positive but PI-negative) and late (annexin-positive and PI-positive) apoptotic cells (Fig. 1A and 1B). We injected GCV into WT mice intraperitoneally after subcutaneous BNL-tk tumor was formed macroscopically, according to the schedule as shown in Fig. 1C. Microscopic analysis revealed that more than half of the tumor cells were apoptotic and that a large number of mononuclear cells had accumulated in the tumor sites on day 19 immediately following the completion of treatment (Fig. 1D and Suppl. Fig. 1). Thereafter, the tumor regressed macroscopically. We next investigated the chemokine receptor expression by tumor-infiltrating cells after the induction of *in vivo* tumor apoptosis by suicide gene therapy. Immunohistochemical analysis revealed the presence of few CCR1-, CCR5-, or CCL3-positive cells in tumors without GCV treatment (Fig. 2A). In contrast, GCV treatment caused intratumoral infiltration of a large number of CCR1-, CCR5-, and CCL3-positive cells in WT mice, along with massive apoptosis of tumor cells (Fig. 2A and Suppl. Fig. 2). The intratumoral mRNA expression of CCL3, CCL4, and CCL5 was markedly increased 3 days after GCV treatment, whereas that of their receptors CCR1 and CCR5 was augmented later than 3 days after GCV injection (Fig. 2B).

Tumor infiltrating DCs express CCR1 and CCR5

In order to determine the type of tumor-infiltrating cells expressing CCR1, CCR5, or CCL3, we performed a double-color immunofluorescence analysis. CD4- and CD8-positive T cells expressed CCR5, but not CCR1 (Fig. 3A and Suppl. Fig. 3A; $78.2 \pm 8.9\%$ of CD4-positive T cells and $92.6 \pm 8.2\%$ of CD8-positive T cells expressed CCR5, and CCR1 was not detected in CD4- or CD8-positive T cells). In contrast, CD11c- and DEC-205-positive cells, which infiltrated to tumor sites of WT mice after GCV treatment, expressed both CCR1 and CCR5 (Fig. 3B and Suppl. Fig. 3B; 100% of CD11c-positive DCs expressed CCR1 and CCR5, $97.5 \pm$

5.6% DEC205-positive cells expressed CCR1 and 100% DEC-positive cells expressed CCR5). Moreover, tumor-infiltrating CD11c-positive DCs exhibited a “myeloid” phenotype because $87.8 \pm 14.8\%$ of CD11c-positive cells expressed CD11b and none of them expressed CD8a (Suppl. Fig. 3C). Furthermore, CCL3 proteins were detected in CD3-positive T cells, F4/80-positive macrophages (Fig. 3C; $72.0 \pm 9.1\%$ of CD3-positive T cells and $87.0 \pm 12.0\%$ of F4/80-positive macrophages expressed CCL3). These observations suggest that apoptosis induced by GCV treatment enhanced the expression of CCL3, CCL4, and CCL5 and then produced chemokines attracted CD11c-positive DCs as well as CD3-positive T cells. In order to address this possibility, we investigated intratumoral infiltration of CD11c-positive DCs and CD3-positive T cells in CCR1KO, CCR5KO, or CCL3KO mice. Mice were subcutaneously inoculated with 2×10^5 BNL-tk cells into WT and knockout mice. The lack of CCR1, CCR5, or CCL3 had no discernible effects on the growth of primary tumors (Fig. 4A). Then, we injected GCV intraperitoneally into the mice as shown in Fig. 1C. Immunohistochemical analysis revealed the presence of few CD3-, F4/80-, or DEC205-positive cells in tumors without GCV treatment (Fig. 4B). GCV treatment induced tumor cell apoptosis in CCL3KO, CCR1KO, and CCR5KO mice to a similar extent as that in WT mice (data not shown). Moreover, GCV treatment caused intratumoral accumulation of a large number of CD3-, CD4-, and CD8-positive T cells, and DEC205- and CD11c-positive DCs in WT mice (Fig. 4B and 4C). By contrast, the increases in intratumorally accumulating DEC205- and CD11c-positive cells and to a lesser extent, CD3-, CD4-, and CD8-positive cells were attenuated in CCR1KO, CCR5KO, and CCL3KO mice (Fig. 4B and 4C). In contrast, GCV treatment induced intratumoral infiltration of F4/80-positive macrophages (Fig. 4B) and CD49b/DX5-positive NK cells (data not shown) in WT and knockout mice to a similar extent.

Partial failure of CCR1KO, CCR5KO, and CCL3KO mice in rejecting the rechallenged tumor

Apoptosis induced by GCV treatment caused intratumoral infiltration of DCs and T cells in a CCR1- and/or CCR5-dependent manner. Because intratumoral infiltration of DCs and T cells is a prerequisite for the establishment of specific tumor immunity, we examined the immune status of GCV-treated mice by rechallenging the parental BNL cell line. In order to completely

eradicate the primary BNL-tk tumor, GCV was administered between 2 and 5 days after the tumor injection (Fig. 5A). Primary BNL-tk tumors were completely eradicated in WT, CCR1KO, CCR5KO, and CCL3KO mice at similar rates (data not shown). When these mice were injected again with parental BNL cells, WT mice completely rejected them. In contrast, CCR1KO, CCR5KO, and CCL3KO mice failed to completely eliminate the rechallenged tumor cells, although the growth rates were retarded in these mice compared with naïve WT mice (Fig. 5B). A marked cytotoxicity against BNL, but not in CT26 cells was observed when draining lymph node-derived mononuclear cells of GCV-treated WT mice were used as effector cells. Only a modest amount of cytotoxicity was detected when mononuclear cells in the draining lymph nodes of GCV-treated CCR1KO, CCR5KO, or CCL3KO mice were used as effector cells (Fig. 5C). Further, GCV-induced tumor apoptosis enhanced the mRNA expression of Th1 cytokines such as IFN- γ , IL-12p40, and IL-18 in the draining lymph nodes of WT mice but not of CCR1KO, CCR5KO, and CCL3KO mice (Suppl. Fig. 4). Likewise, CD8⁺IFN- γ ⁺ cells were markedly increased in GCV-treated WT mice when lymph node-derived mononuclear cells were co-cultured with BNL cell lysates, compared with tumor-bearing or tumor-free WT mice (Fig. 5D). Increases in CD8⁺IFN- γ ⁺ cells were less evident in CCR1KO, CCR5KO, or CCL3KO mice treated with tumor cells and GCV compared with WT mice when lymph node-derived cells were co-cultured with BNL cell lysates (Fig. 5D). These observations suggest that the absence of CCR1, CCR5, or CCL3 greatly impaired the apoptosis-induced establishment of specific tumor immunity.

Apoptosis-induced migration of DCs to draining lymph nodes and intranodal T cell proliferation activation in a CCR1-, CCR5-, and/or CCL3-dependent manner

Tumor-infiltrating DCs can uptake tumor antigens at the tumor sites and migrate to the draining lymph nodes, where they mature to present antigens to T cells (17, 18). Thus, we further explored the status of DCs as well as T cells in the draining lymph nodes. Following GCV treatment, tumor apoptosis increased the proportions of CD86⁺CD11c⁺ cells in the draining lymph nodes but not in distant lymph nodes in WT mice (Fig. 6A). In contrast, GCV-induced increases in CD11c⁺ cell proportion were depressed in CCR1KO, CCR5KO, or CCL3KO mice (Fig. 6A). The levels of CD86 on CD11c⁺ cells were increased in GCV-treated WT mice

compared with WT mice, which had been injected with neither BNL-tk cells nor GCV, although the levels of CD86 were depressed in the knockout mice (mean fluorescent intensities of CD86 on CD11c⁺ cells: WT/BNL-tk/GCV, 114.3 ± 8.6 ; WT/BNL-tk, 86.2 ± 12.2 ; WT/no tumor, 86.5 ± 2.6 ; CCR1KO/BNL-tk/GCV, 85.4 ± 15.6 ; CCR5KO/BNL-tk/GCV, 92.3 ± 12.6 ; CCL3KO/BNL-tk/GCV, 79.0 ± 9.8). Moreover, GCV-induced tumor apoptosis increased significantly the numbers of total cells, CD4⁺ and CD8⁺ cells in the draining lymph nodes of WT mice. GCV-induced increases in these cell populations were also attenuated in CCR1KO, CCR5KO, or CCL3KO mice (Fig. 6B). Lymphocytes expressing the cell proliferation marker Ki67 were increased in the paracortical areas of the draining lymph nodes of GCV-treated WT mice compared with the other groups (Fig. 6C and Suppl. Fig. 5). Injection of BNL-tk cells increased marginally the proportion of activated CD4⁺ T cells, defined as CD44^{hi}CD62L^{lo}CD4⁺, in the draining lymph nodes. Co-injection of GCV further augmented this increment in WT mice but not in knockout mice (Fig. 6D and E). These observations suggest that the absence of CCR1, CCR5, or CCL3 impaired the GCV-induced migration of DCs into the draining lymph nodes and the subsequent proliferation and activation of T cells in the draining lymph nodes.

Restoration of anti-tumor response of knockout mice by adoptive transfer of DCs harvested from GCV-treated WT mice

Given the proposed crucial role of DCs in evoking antitumor immunity after tumor apoptosis, we finally performed adoptive transfer of DCs harvested from the draining lymph nodes of GCV-treated WT mice into the knockout mice. DCs were harvested from the draining lymph nodes of GCV-treated tumor-bearing or tumor-free WT mice, and were transferred subcutaneously into the knockout mice on day 8 (Fig. 5A). The knockout mice completely rejected the rechallenged cells when DCs were transferred from GCV-treated tumor-bearing WT mice, but not tumor-free WT mice (Fig. 7). These observations suggest that GCV-induced tumor apoptosis mediated the trafficking of DCs to the draining lymph nodes, which can induce the establishment of specific immunity in a CCR1-, CCR5-, or CCL3-dependent manner.

DISCUSSION

Apoptosis was previously presumed to be immunologically silent or even tolerogenic (27). However, recent reports have indicated that tumor cell apoptosis can induce antitumor immune responses effectively because the immunogenicity of apoptotic tumor cells is dependent on apoptosis inducers. Indeed, gemcitabine-induced apoptosis can augment cross-priming of tumor-specific CD8⁺ T cells *in vivo* rather than cross-tolerizing (8). Similarly, apoptosis induced by local radiation therapy can generate tumor antigen-specific effector cells that migrate to the tumor (28). Moreover, apoptotic change caused by anthracyclin can induce the translocation of calreticulin to the apoptotic tumor cell surface, and calreticulin exposure can enhance the immunogenicity of apoptotic cancer cells (6, 7). Thus, apoptosis induced by these measures are sufficiently immunogenic to prevent tumor progression.

The combination of HSV-tk gene transfer and GCV can efficiently induce the apoptosis of the transfected tumors as observed in the present study. Here, we also observed that the treatment augmented the immune response as evidenced by an increase in the number of tumor-infiltrating DCs. Subsequently, the number of DCs in the draining lymph nodes increased together with enhanced specific immunity to the injected tumor. These observations suggest that tumor apoptosis induced by HSV-tk/GCV treatment are effective in generating specific tumor immunity, similar to that observed in the case of anti-cancer drug treatment.

Consistent with our present observations, CCL3 and its related chemokine CCL5 were detected in macrophages infiltrating human cancer tissues (29, 30). Given their potent chemotactic activity against various types of immune cells (31), gene transfer of CCL3 or CCL5 induced the accumulation of immune cells including DCs, T cells, macrophages, and NK cells in the tumor sites, resulting in delayed tumor growth and prolonged survival (16, 32-34). Moreover, combination therapy of HSV-tk and CCL3/CCL20 gene induces an exaggerated accumulation of DCs, CD4⁺ cells, CD8⁺ cells, NK cells, and macrophages in the tumor sites, compared with HSV-tk/GCV treatment alone and the net effects are tumor regression and prolonged survival (34). However, the roles of endogenously produced CCL3 and its related chemokines in tumor apoptosis still remain to be elucidated.

In human HCC, tumor-infiltrating lymphocytes express high levels of CCR5 and

CXCR3. Moreover, these lymphocytes show strong chemotactic responses to both CC and CXC chemokines including CCL3, CCL4, and CXCL9 (35). Additional treatments are nevertheless required to enhance the immune responses because the CCR5- or CXCR3- positive lymphocytes are insufficient to evoke immune responses and eradicate tumor tissues. We demonstrated that suicide gene therapy-induced tumor cell apoptosis augments CCR1- and CCR5-positive cell infiltration into the hepatoma tissues. Further, these CCR1- or CCR5-positive cells are DCs and/or T cells, the cells indispensable for tumor immunity. Thus, suicide gene therapy can potentially enhance tumor immunity by attracting these immune cells to the apoptotic tumor cells.

The initial step leading to specific tumor immunity is the capture of tumor antigens by macrophages and immature DCs, both of which accumulate in tumor sites. However, in this model, CCR1KO, CCR5KO, and CCL3KO mice failed to completely eliminate the rechallenged tumor cells along with reduced intratumoral accumulation of DCs but not F4/80-positive macrophages. These observations suggest that the establishment of specific tumor immunity requires intratumoral recruitment of immature DCs but not macrophages. Activated NK cells can also induce DC maturation in lymphoid organs as well as in non-lymphoid tissues. Although NK cells express chemokine receptors such as CCR5 (36), the deficiency of CCR1 or CCR5 has little effects on intratumoral infiltration of NK cells. These observations preclude the crucial role of NK cells in the establishment of specific tumor immunity in this model.

Immature DCs utilize several chemokine receptors including CCR1, CCR2, CCR4, CCR5, CCR6, CCR8, and CXCR4, for their migration (22). However, the chemokine receptor(s) regulating immature DC trafficking to tumor sites still need(s) to be determined. We previously observed that CCL3 induced mobilization of dendritic cell precursors into circulation (37) and detected CCL3 in tumor-infiltrating CD3⁺ T cells and macrophages after GCV treatment. Therefore, we investigated the roles of CCL3 and its receptors, CCR1 and CCR5, in the intratumoral recruitment of DCs and the subsequent establishment of specific tumor immunity. Although CCL4 and CCL5 expression was augmented along with CCL3 expression in tumor sites, the deletion of *CCL3* gene alone reduced markedly the DC migration, intranodal T cell accumulation, and subsequent Th1 cytokine expression. Similarly, deletion of *CCL3* gene

alone prevented coxsackievirus-induced myocarditis (38), despite enhanced intracardiac expression of CCL3, CCL4, and CCL5 mRNA (39). Thus, these three chemokines may form a positive feedback loop and the deletion of either chemokine might reduce the expression of the others. Moreover, the lack of CCR1 or CCR5 reduces the migration of DCs to tumor sites and subsequent tumor immunity in the draining lymph nodes, such as DC and T cell accumulation, and Th1 cytokine expression. Because almost all CD11c- and DEC205-positive DCs express both CCR1 and CCR5, DC migration may require coordinated and synergistic actions of both these chemokine receptors.

We have provided definitive evidence regarding the essential contribution of CCL3 and its receptors to apoptosis-induced specific tumor immunity, which exert their role by attracting DCs to tumor tissues. These observations further suggest that specific tumor immunity can be more efficiently established if some techniques such as chemokine gene transfer can augment the recruitment of immature DCs to apoptotic tumor tissues caused by chemotherapeutic agents and/or irradiation as well as suicide gene therapy.

ACKNOWLEDGMENTS

We thank Dr. Philip M. Murphy (NIAID, NIH, Bethesda, MD) for providing us with CCR1-deficient mice. We also thank Dr. Toshikazu Kondo (Wakayama Medical University, Wakayama, Japan) for his technical advice on double-color immunofluorescence analysis.

REFERENCES

1. Tsukuma, H., Hiyama, T., Tanaka, S., Nakao, M., Yabuuchi, T., Kitamura, T., Nakanishi, K., Fujimoto, I., Inoue, A., Yamazaki, H., Kawashima, T. (1993) Risk factors for hepatocellular carcinoma among patients with chronic liver disease. *N. Engl. J. Med.* 328, 1797-1801.
2. Velázquez, R. F., Rodríguez, M., Navascués, C. A., Linares, A., Pérez, R., Sotorríos, N. G., Martínez, I., Rodrigo, L. (2003) Prospective analysis of risk factors for hepatocellular carcinoma in patients with liver cirrhosis. *Hepatology.* 37, 520-527.
3. Okita, K. (2006) Management of hepatocellular carcinoma in Japan. *J. Gastroenterol.* 41, 100-106.
4. Poon, R. T., Fan, S. T., Ng, I. O., Lo, C. M., Liu, C. L., Wong, J. (2000) Different risk factors and prognosis for early and late intrahepatic recurrence after resection of hepatocellular carcinoma. *Cancer.* 89, 500-507.
5. Butterfield, L. H. (2004) Immunotherapeutic strategy for hepatocellular carcinoma. *Gastroenterology.* 127, S232-S241.
6. Obeid, M., Tesniere, A., Ghiringhelli, F., Fimia, G. M., Apetoh, L., Perfettini, J. L., Castedo, M., Mignot, G., Panaretakis, T., Casares, N., Métivier, D., Larochette, N., van Endert, P., Ciccosanti, F., Piacentini, M., Zitvogel, L., Kroemer, G. (2007) Calreticulin exposure dictates the immunogenicity of cancer cell death. *Nat. Med.* 13, 54-61.
7. Casares, N., Pequignot, M. O., Tesniere, A., Ghiringhelli, F., Roux, S., Chaput, N., Schmitt, E., Hamai, A., Hervas-Stubbs, S., Obeid, M., Coutant, F., Métivier, D., Pichard, E., Aucouturier, P., Pierron, G., Garrido, C., Zitvogel, L., Kroemer, G. (2005) Caspase-dependent immunogenicity of doxorubicin-induced tumor cell death. *J. Exp. Med.* 202, 1691-1701.
8. Nowak, A. K., Lake, R. A., Marzo, A. L., Scott, B., Heath, W. R., Collins, E. J., Frelinger, J. A., Robinson, B. W. S. (2003) Induction of tumor cell apoptosis in vivo increases tumor antigen cross-presentation, cross-priming rather than cross-tolerizing host tumor-specific CD8 T cells. *J. Immunol.* 170, 4905-4913.
9. Hamel, W., Magnelli, L., Chiarugi, V. P., Israel, M. A. (1996) Herpes simplex virus thymidine kinase/ganciclovir-mediated apoptotic death of bystander cells. *Cancer Res.* 56,

2697-2702.

10. Beltinger, C., Fulda, S., Kammertoens, T., Meyer, E., Uckert, W., Debatin, K. M. (1999) Herpes simplex virus thymidine kinase/ganciclovir-induced apoptosis involves ligand-independent death receptor aggregation and activation of caspases. *Proc. Natl. Acad. Sci. USA.* 96, 8699-8704.
11. Freeman, S. M., Ramesh, R., Marrogi, A. J. (1997) Immune system in suicide-gene therapy. *Lancet.* 349, 2-3.
12. Vile, R. G., Castleden, S., Marshall, J., Camplejohn, R., Upton, C., Chong, H. (1997) Generation of an anti-tumour immune response in a non-immunogenic tumour: HSVtk killing *in vivo* stimulates a mononuclear cell infiltrate and a Th1-like profile of intratumoural cytokine expression. *Int. J. Cancer.* 71, 267-274.
13. Freeman, S. M., Ramesh, R., Shastri, M., Munshi, A., Jensen, A. K., Marrogi, A. J. (1995) The role of cytokines in mediating the bystander effect using HSV-TK xenogeneic cells. *Cancer Lett.* 92, 167-174.
14. Chen, S. H., Chen, X. H. L., Wang, Y., Kosai, K., Finegold, M. J., Rich, S. S., Woo, S. L. C. (1995) Combination gene therapy for liver metastasis of colon carcinoma *in vivo*. *Proc. Natl. Acad. Sci. USA.* 92, 2577-2581.
15. Chen, S. H., Kosai, K., Xu, B., Pham-Nguyen, K., Contant, C., Finegold, M. J., Woo, S. L. C. (1996) Combination suicide and cytokine gene therapy for hepatic metastases of colon carcinoma: sustained antitumor immunity prolongs animal survival. *Cancer Res.* 56, 3758-3762.
16. Tsuchiyama, T., Nakamoto, Y., Sakai, Y., Marukawa, Y., Kitahara, M., Mukaida, N., Kaneko, S. (2007) Prolonged, NK cell-mediated antitumor effects of suicide gene therapy combined with monocyte chemoattractant protein-1 against hepatocellular carcinoma. *J. Immunol.* 178, 574-583.
17. Banchereau, J., Steinman, R. M. (1998) Dendritic cells and the control of immunity. *Nature.* 392, 245-252.
18. Sallusto, F., Lanzavecchia, A. (1999) Mobilizing dendritic cells for tolerance, priming, and chronic inflammation. *J. Exp. Med.* 189, 611-614.
19. Castellino, F., Huang, A. Y., Altan-Bonnet, G., Stoll, S., Scheinecker, C., Germain, R. N.

- (2006) Chemokines enhance immunity by guiding naïve CD8⁺ T cells to sites of CD4⁺ T cell-dendritic cell interaction. *Nature*. 440, 890-895.
20. Dieu, M.C., Vanbervliet, B., Vicari, A., Bridon, J. M., Oldham, E., Aït-Yahia, S., Brière, F., Zlotnik, A., Lebecque, S., Caux, C. (1998) Selective recruitment of immature and mature dendritic cells by distinct chemokines expressed in different anatomic sites. *J. Exp. Med.* 188, 373-386.
21. Sozzani, S., Luini, W., Borsatti, A., Polentarutti, N., Zhou, D., Piemonti, L., D'Amico, G., Power, C. A., Wells, T. N. C., Gobbi, M., Allavena, P., Mantovani, A. (1997) Receptor expression and responsiveness of human dendritic cells to a defined set of CC and CXC chemokines. *J. Immunol.* 159, 1993-2000.
22. Sozzani, S. (2005) Dendritic cell trafficking: more than just chemokines. *Cytokine Growth Factor Rev.* 16, 581-592.
23. Murai, M., Yoneyama, H., Ezaki, T., Suematsu, M., Terashima, Y., Harada, A., Hamada, H., Asakura, H., Ishikawa, H., Matsushima, K. (2003) Peyer's patch is the essential site in initiating murine acute and lethal graft-versus-host reaction. *Nat. Immunol.* 4, 154-160.
24. Tsuchiyama, T., Kaneko, S., Nakamoto, Y., Sakai, Y., Honda, M., Mukaida, N., Kobayashi, K. (2003) Enhanced antitumor effects of a bicistronic adenovirus vector expressing both herpes simplex virus thymidine kinase and monocyte chemoattractant protein-1 against hepatocellular carcinoma. *Cancer Gene. Ther.* 10, 260-269.
25. Murai, M., Yoneyama, H., Harada, A., Yi, Z., Vestergaard, C., Guo, B., Suzuki, K., Asakura, H., Matsushima, K. (1999) Active participation of CCR5⁺CD8⁺ T lymphocytes in the pathogenesis of liver injury in graft-versus-host disease. *J. Clin. Invest.* 104, 49-57.
26. Lu, P., Nakamoto, Y., Nemoto-Sakai, Y., Fujii, C., Wang, H., Hashii, M., Ohmoto, Y., Kaneko, S., Kobayashi, K., Mukaida, N. (2003) Potential interaction between CCR1 and its ligand, CCL3, induced by endogeneously produced interleukin-1 in human hepatomas. *Am. J. Pathol.* 162, 1249-1258.
27. Steinman, R. M., Turley, S., Mellman, I., Inaba, K. (2000) The induction of tolerance by dendritic cells that have captured apoptotic cells. *J. Exp. Med.* 191, 411-416.
28. Lugade, A. A., Moran, J. P., Gerber, S. A., Rose, R. C., Frelinger, J. G., Lord, E. M. (2005) Local radiation therapy of B16 melanoma tumors increases the generation of tumor

- antigen-specific effector cells that traffic to the tumor. *J. Immunol.* 174, 7516-7523.
29. Tang, K. F., Tan, S. Y., Chan, S. H., Chong, S. M., Loh, K. S., Tan, L. K. S., Hu, H. (2001) A distinct expression of CC chemokines by macrophages in nasopharyngeal carcinoma: implication for the intense tumor infiltration by T lymphocytes and macrophages. *Hum. Pathol.* 32, 42-49.
 30. Musha, H., Ohtani, H., Mizoi, T., Kinouchi, M., Nakayama, T., Shiiba, K., Miyagawa, K., Nagura, H., Yoshie, O., Sasaki, I. (2005) Selective infiltration of CCR5⁺CXCR3⁺ T lymphocytes in human colorectal carcinoma. *Int. J. Cancer.* 116, 949-956.
 31. Menten, P., Wuyts, A., van Damme, J. (2002) Macrophage inflammatory protein-1. *Cytokine Growth Factor Rev.* 13, 455-481.
 32. Lavergne, E., Combadière, C., Iga, M., Boissonnas, A., Bonduelle, O., Maho, M., Debré, P., Combadière, B. (2004) Intratumoral CC chemokine ligand 5 overexpression delays tumor growth and increases tumor cell infiltration. *J. Immunol.* 173, 3755-3762.
 33. Fushimi, T., Kojima, A., Moore, M. A., Crystal, R. G. (2000) Macrophage inflammatory protein 3 α transgene attracts dendritic cells to established murine tumors and suppresses tumor growth. *J. Clin. Invest.* 105, 1383-1393.
 34. Crittenden, M., Gough, M., Harrington, K., Olivier, K., Thompson, J., Vile, R. G. (2003) Expression of inflammatory chemokines combined with local tumor destruction enhances tumor regression and long-term immunity. *Cancer Res.* 63, 5505-5512.
 35. Yoong, K. F., Afford, S. C., Jones, R., Aujla, P., Qin, S., Price, K., Hubscher, S. G., Adams, D. H. (1999) Expression of CXC and CC chemokines in human malignant liver tumors: a role for human monokine induced by γ -interferon in lymphocyte recruitment to hepatocellular carcinoma. *Hepatology.* 30, 100-111.
 36. Walzer, T., Dalod, M., Robbins, S. H., Zitvogel, L., Vivier, E. (2005) Natural-killer cells and dendritic cells: "l'union fait la force" *Blood.* 106, 2252-2258.
 37. Zhang, Y., Yoneyama, H., Wang, Y., Ishikawa, S., Hashimoto, S., Gao, J. L., Murphy, P. M., Matsushima, K. (2004) Mobilization of dendritic cell precursors into the circulation by administration of MIP-1 α in mice. *J. Natl. Cancer Inst.* 96, 201-209.
 38. Cook, D. N., Beck, M. A., Coffman, T. M., Kirby S. L., Sheridan, J. F., Pragnell, I. B., Smithies, O. (1995) Requirement for an inflammatory response to viral infection. *Science*

269, 1583-1585.

39. Gebhard, J. R., Perry, C. M., Harkins, S., Lane, T., Mena, I., Asensio, V. C., Campbell, I. L., Whitton, J. L. (1998) Coxsackievirus B3-induced myocarditis. Perforin exacerbates disease, but plays no detectable role in virus clearance. *Am. J. Pathol.* 153, 41-428.

FIGURE LEGENDS

Figure 1

Apoptosis of murine hepatoma cell line induced by GCV treatment. After 1 day of culture without (A) or with (B) 5 $\mu\text{g/ml}$ GCV, BNL-tk cells were harvested and stained with the Annexin V-FITC Apoptosis Detection Kit and propidium iodide. Then, the cells were analyzed by flow cytometry. Representative results from 3 individual experiments are shown here. (C) Schematic representation of GCV treatment *in vivo*. Mice were subcutaneously injected with 2×10^5 BNL-tk cells on day 0. Then, GCV was intraperitoneally injected into mice from days 14 to 18. Tumors were harvested on the day before GCV injection (day 13), on day 3 or 6 after GCV injection (day 16 or 19) for real-time RT-PCR analysis, and on day 19 for immunohistochemistry (IHC). (D) Apoptotic cells detected in tumor tissues with or without GCV treatment using anti-ssDNA antibody. Original magnification, $\times 400$. Bar, 50 μm .

Figure 2

Accumulation of tumor-infiltrating CCR1-, CCR5-, or CCL3-positive cells after tumor apoptosis induced by GCV treatment. Mice were inoculated with BNL-tk cells according to the schedule shown in Fig. 1C. (A) Tumors were removed from WT mice on day 19 and immunohistochemical analysis was performed using anti-CCR1, anti-CCR5, or anti-CCL3 antibody on tumors with or without GCV treatment. Representative results from 3 individual animals in each group are shown here. Original magnification, $\times 400$. Bars, 50 μm . (B) Real-time RT-PCR was performed on total RNA extracted from the tumor of WT mice harvested on day 13, 16, or 19. The level of chemokine mRNA was normalized to GAPDH mRNA levels. Bars, ± 1 SD ($n = 3$); *, $p < 0.05$ compared with the day before GCV injection.

Figure 3

Identification of CCR1-, CCR5-, and CCL3-expressing cells in the tumor sites. Mice were inoculated with BNL-tk cells according to the schedule shown in Fig. 1C. (A), (B), and (C) Tumors were removed from WT mice on day 19 and immunostained with the indicated combinations of antibodies as described in Materials and Methods. The digitally merged images

are shown in the right panels. Representative results from 3 individual animals are shown. Original magnification, $\times 400$. Bars, $50 \mu\text{m}$.

Figure 4

Deficiency of CCR1, CCR5, or CCL3 impaired intratumoral accumulation of DCs and T cells after tumor apoptosis induced by GCV treatment. Mice were inoculated with BNL-tk cells according to the schedule shown in Fig. 1C. (A) WT and knockout mice were inoculated with 2×10^5 BNL-tk cells. The sizes of primary tumors were measured without GCV treatment and shown here. Bars, ± 1 SE. (B) The numbers of CD3-, CD4-, CD8-, F4/80-, DEC205-, or CD11c-positive cells were enumerated from the tumors harvested from mice with or without GCV. The cell density was determined in 10 randomly chosen tumor areas at 400-fold magnification. Bars, ± 1 SD. *, $p < 0.05$ compared with WT. (C) Immunohistochemical analysis was performed using anti-CD3, anti-DEC205, or anti-CD11c antibody on tumors after GCV treatment in WT and knockout mice. Representative results from 3 individual animals in each group are shown here. Original magnification, $\times 400$. Bars, $50 \mu\text{m}$.

Figure 5

Partial failure of CCR1KO, CCR5KO, and CCL3KO mice in rejecting the rechallenged tumor. (A) Schematic representation of the treatment schedule. Mice were subcutaneously injected with 1.5×10^5 BNL-tk cells on day 0. GCV was intraperitoneally injected into mice from days 2 to 5. Following complete eradication of the primary tumors, the mice were subcutaneously rechallenged with 1.0×10^5 BNL cells on day 18. (B) Tumor sizes were measured twice a week and are shown here. Bars, ± 1 SE; *, $p < 0.05$. WT mice, which had been injected with neither BNL-tk cells nor GCV beforehand, were injected with BNL cells and are shown here as control. (C) Mononuclear cells from the draining lymph nodes (DLN) on day 8, were incubated at a cell density of 2×10^6 cells/ml in the presence of 0.6×10^6 cells/ml BNL cells, which were irradiated at 50 Gy beforehand. After 5 days of culture, the cells were tested for *in vitro* cytotoxicity against BNL or CT26 cells as a control as described in Materials and Methods. Each value represents mean ± 1 SE ($n = 3$). (D) Mononuclear cells from DLN on day 8 were incubated for 6 h with the lysates of BNL or CT26 cells, and stained with CD8 antibody and

IFN- γ antibody or isotype control as described in Materials and Methods. The cells were analyzed by flow cytometry and the percentages of CD8⁺IFN- γ ⁺ cells of CD8⁺ cells are indicated in the right corners. Representative results from 3 individual animals are shown here.

Figure 6

Apoptosis-induced migration of DCs to the draining lymph nodes (DLN) and intranodal T cell proliferation and activation in CCR1-, CCR5-, and/or CCL3-dependent manner. Mice were treated according to the schedule shown in Fig. 5A. (A) DLN or distal lymph nodes (distal LN) were harvested on day 8 as indicated in Fig. 5A. Mononuclear cells were stained with a combination of FITC-labeled anti-CD86 and PE-labeled anti-CD11c antibodies. The percentage of CD11c⁺CD86⁺ cells was determined and is indicated in the right corners. Representative results from 3 individual animals are shown here. (B) Absolute cell numbers of each cell population in the DLN or distal LN on day 8 were determined as described in Materials and Methods. Bars, ± 1 SD; *, $p < 0.05$ compared with DLN derived from WT mice treated with BNL-tk/GCV. (C) DLN harvested on day 8 were immunostained with anti-Ki67 antibody and percentages of Ki67⁺ cells in lymph nodes were determined. Bars, ± 1 SD; *, $p < 0.05$ compared with DLN derived from WT mice treated with BNL-tk/GCV. (D) and (E) Mononuclear cells harvested on day 8 were stained with a combination of FITC-labeled anti-CD4 and PE-labeled anti-CD44 (D) or PE-labeled anti-CD62L (E) antibodies. Histograms were gated on CD4-positive cells and percentages of CD44^{hi} (D) or CD62L^{lo} (E) cells were determined. Representative results from 3 individual animals are shown here.

Figure 7

Adoptive transfer of DCs harvested from GCV-treated WT mice restored the antitumor response of knockout mice. After inoculation of BNL-tk tumors, CCR1KO, CCR5KO, or CCL3KO mice were treated with GCV from days 2 to 5 as described in Fig. 5A. The DCs were then harvested from the draining lymph nodes of GCV-treated WT mice and transferred subcutaneously into the knockout mice on day 8 as shown in Fig. 5A. On day 18, these mice were injected again with parental BNL cells, and tumor sizes were measured on day 28. GCV-treated knockout mice

transferred without or with DCs of naïve WT mice were also rechallenged with parental BNL cells, as control. Bars, mean; *, $p < 0.05$.

Supplemental Figure 1

As a control for Fig. 1D, normal rabbit IgG was used instead of rabbit anti-ssDNA antibody. Original magnification, $\times 400$. Bar, 50 μm .

Supplemental Figure 2

As a control for Fig. 2A, normal goat or rabbit IgG was used instead of goat anti-CCR1 antibody, goat anti-CCL3 antibody, or rabbit anti-CCR5 antibody. Original magnification, $\times 400$. Bar, 50 μm .

Supplemental Figure 3

Tumors were removed from WT mice on day 19 (Fig. 1C) and were immunostained with the indicated combinations of antibodies as described in Materials and Methods. The digitally merged images are shown in the right panels. Representative results from 3 individual animals are shown here. Original magnification, $\times 400$. Bars, 50 μm .

Supplemental Figure 4

Mice were treated according to the schedule as shown in Fig. 5A. (A) and (B) RT-PCR was performed on total RNA extracted from DLN that was harvested from mice on day 8. Representative results from 3 individual experiments are shown in A. The ratios of intensities of cytokines to GAPDH were calculated by assuming the ratio of WT mice treated with GCV as 1.0 and are shown in B. Bars, ± 1 SD ($n = 3$); *, $p < 0.05$ compared with WT/BNL-tk/GCV.

Supplemental Figure 5

Draining lymph nodes were harvested on day 8 (Fig. 5A) and were immunostained with anti-Ki67 antibody. Representative results from 3 individual animals in each group are shown here. Original magnification, $\times 400$. Bars, 50 μm .

Figure 1

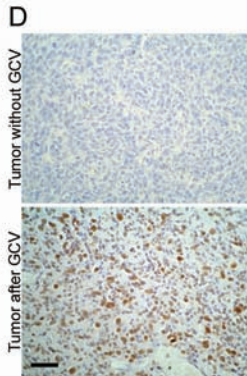
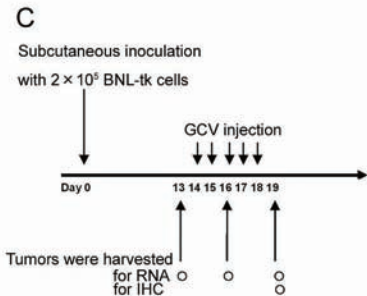
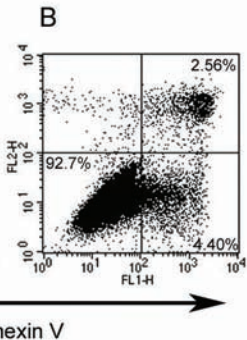
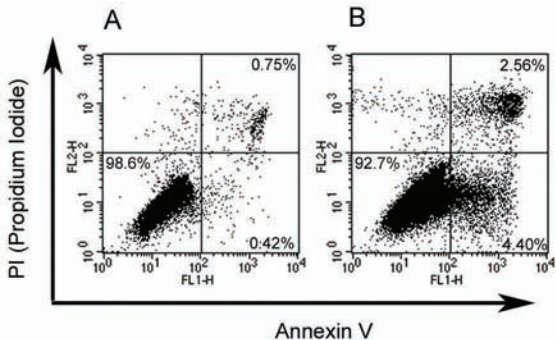


Figure 2

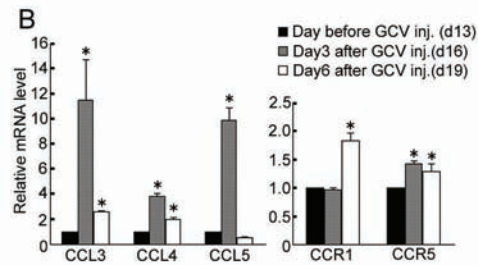
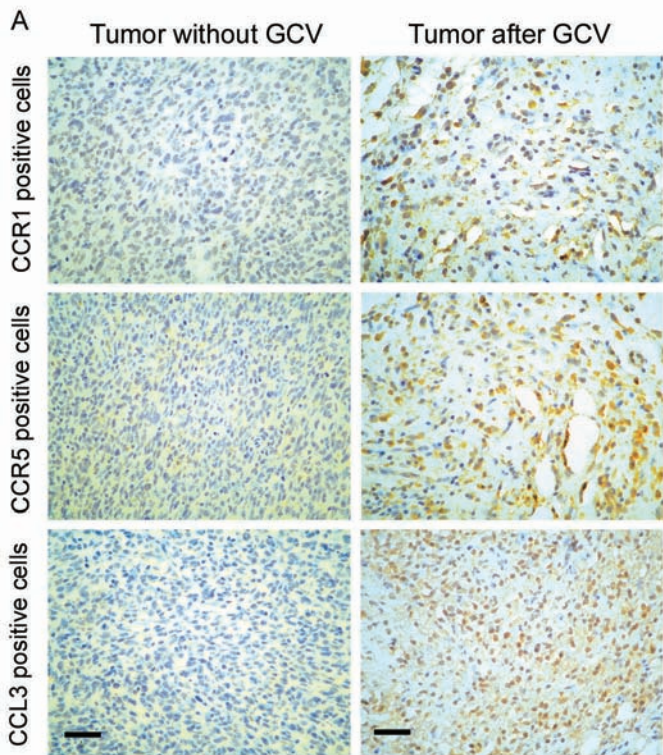
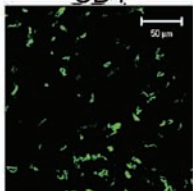


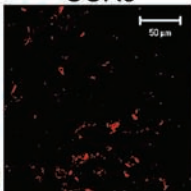
Figure 3

A

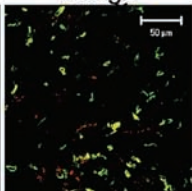
CD4



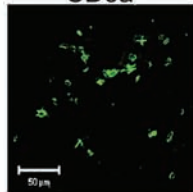
CCR5



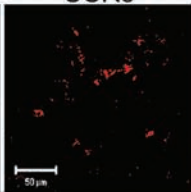
Merge



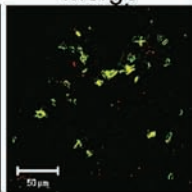
CD8a



CCR5

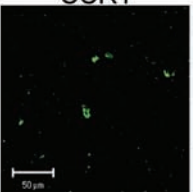


Merge

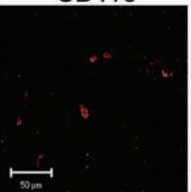


B

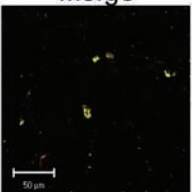
CCR1



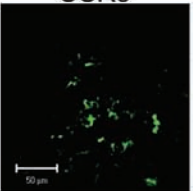
CD11c



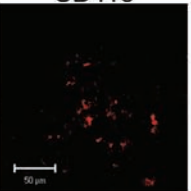
Merge



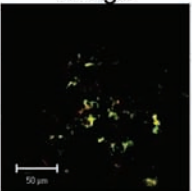
CCR5



CD11c

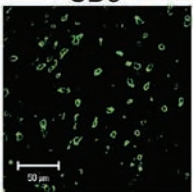


Merge

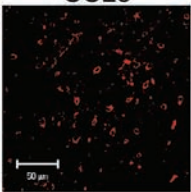


C

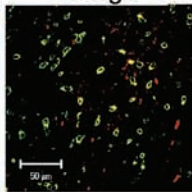
CD3



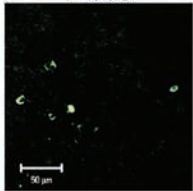
CCL3



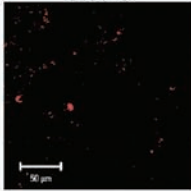
Merge



F4/80



CCL3



Merge

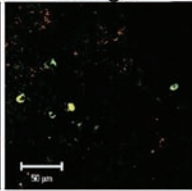


Figure 4

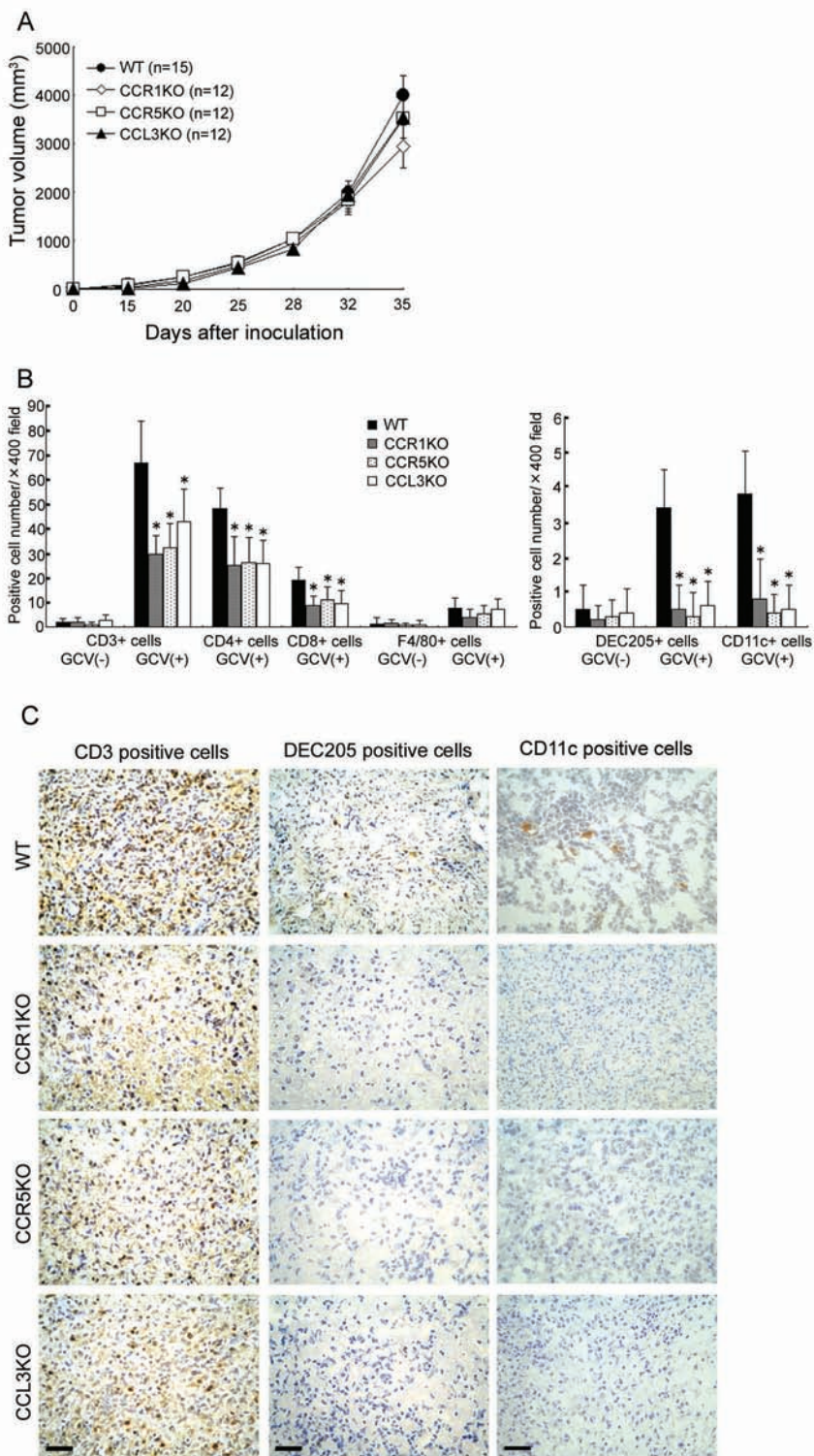


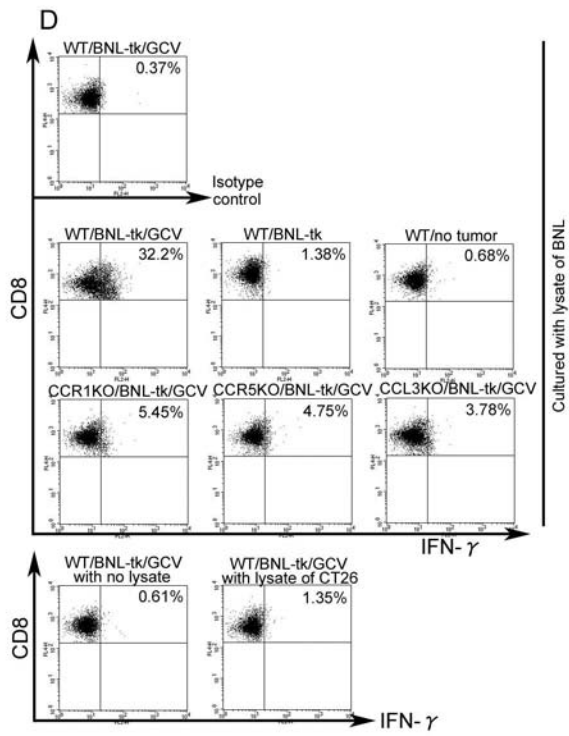
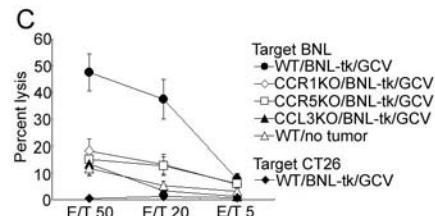
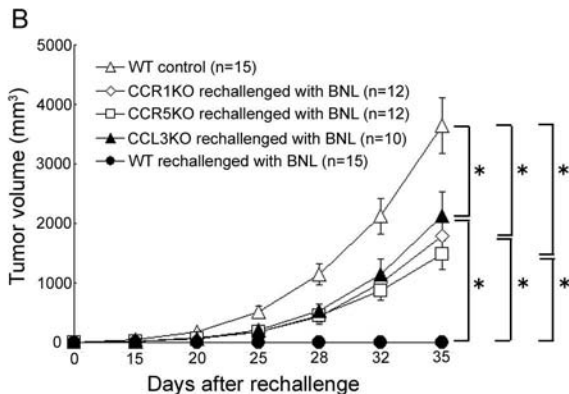
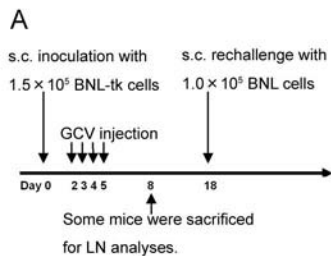
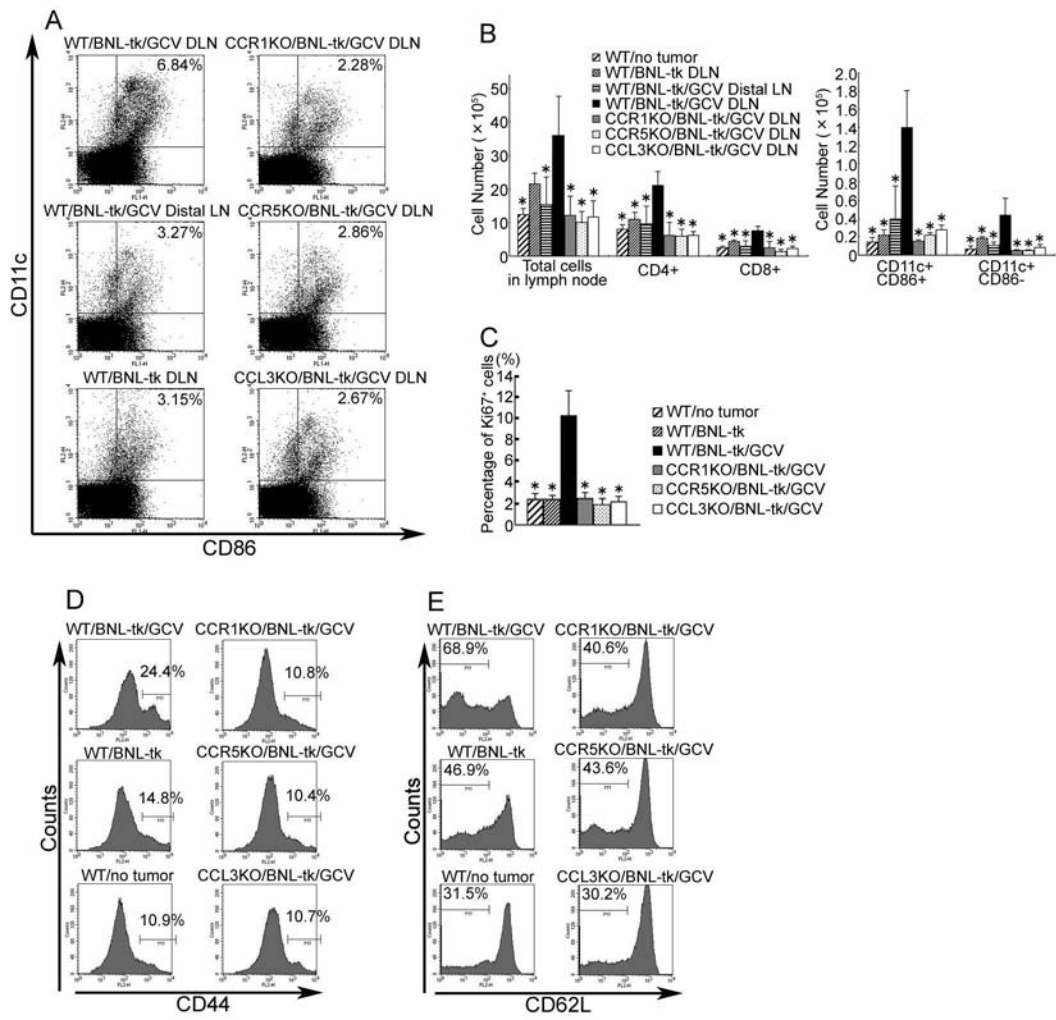
Figure 5

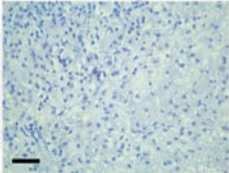
Figure 6



Supplemental Figure 1

Rabbit IgG

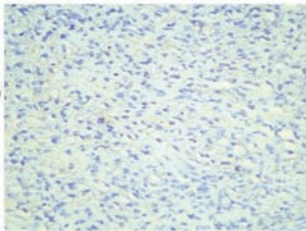
Tumor after GCV



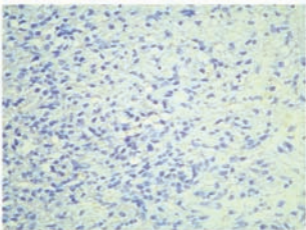
Supplemental Figure 2

Tumor after GCV

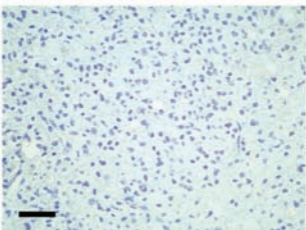
Goat IgG



Rabbit IgG



Goat IgG



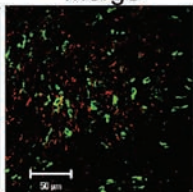
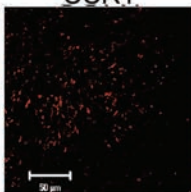
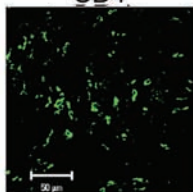
Supplemental Figure 3

A

CD4

CCR1

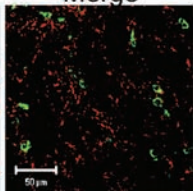
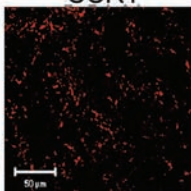
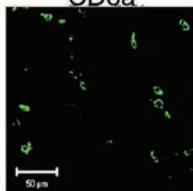
Merge



CD8a

CCR1

Merge

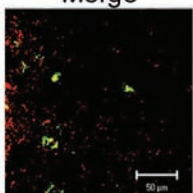
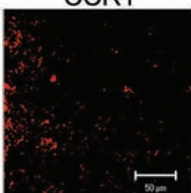
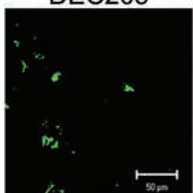


B

DEC205

CCR1

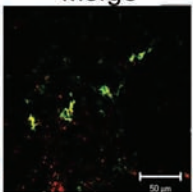
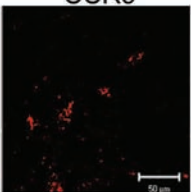
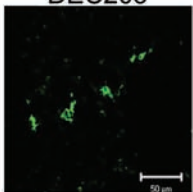
Merge



DEC205

CCR5

Merge

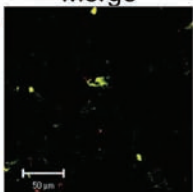
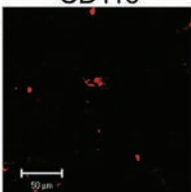
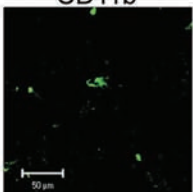


C

CD11b

CD11c

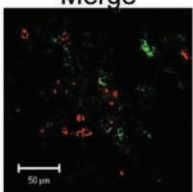
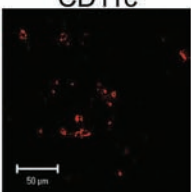
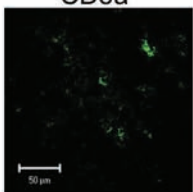
Merge



CD8a

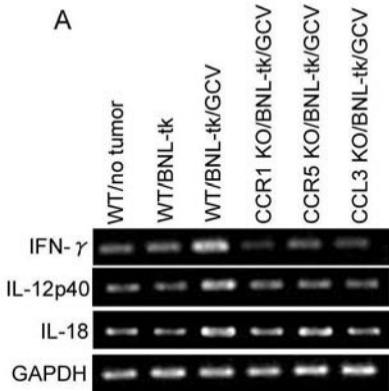
CD11c

Merge

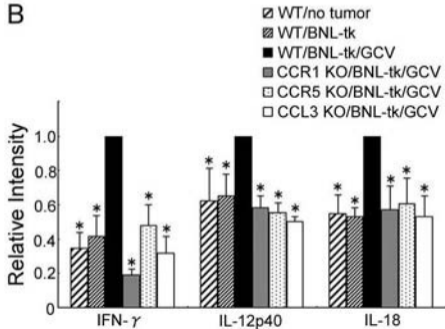


Supplemental Figure 4

A



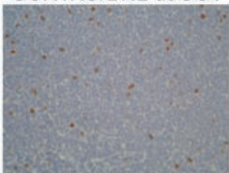
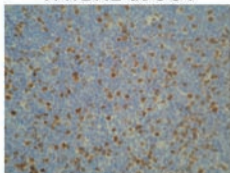
B



Supplemental Figure 5

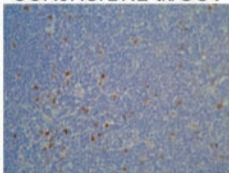
WT/BNL-tk/GCV

CCR1KO/BNL-tk/GCV



WT/BNL-tk

CCR5KO/BNL-tk/GCV



WT/no tumor

CCL3KO/BNL-tk/GCV

